Published in final edited form as:
Traffic. 2011 March ; 12(3): 330–348. doi:10.1111/j.1600-0854.2010.01149.x.

Alzheimer's disease-associated ubiquilin-1 regulates presenilin-1 accumulation and aggresome formation

Jayashree Viswanathan[1,*], **Annakaisa Haapasalo**[1,*], **Claudia Böttcher**[2], **Riitta Miettinen**[1,3], **Kaisa M.A. Kurkinen**[1], **Alice Lu**[4], **Anne Thomas**[5], **Christa J. Maynard**[2], **Donna Romano**[4], **Bradley T. Hyman**[5], **Oksana Berezovska**[5], **Lars Bertram**[6], **Hilkka Soininen**[1], **Nico P. Dantuma**[2], **Rudolph E. Tanzi**[4], and **Mikko Hiltunen**[1,§]

[1]Institute of Clinical Medicine - Neurology, University of Eastern Finland and Department of Neurology, Kuopio University Hospital, Kuopio, Finland [2]Department of Cell and Molecular Biology, Karolinska Institutet, Stockholm, Sweden [3]CNServices Ltd, Kuopio, Finland [4]Genetics and Aging Research Unit, Massachusetts General Hospital/Harvard Medical School, Charlestown, MA, USA [5]Alzheimer's Research Unit, MassGeneral Institute for Neurodegenerative Disease, Massachusetts General Hospital, Charlestown [6]Department of Vertebrate Genomics, Max-Planck-Institute for Molecular Genetics, Berlin, Germany

Abstract

The Alzheimer's disease (AD)-associated ubiquilin-1 regulates proteasomal degradation of proteins, including presenilin (PS). PS-dependent γ-secretase generates β-amyloid (Aβ) peptides, which excessively accumulate in AD brain. Here we have characterized the effects of naturally occurring ubiquilin-1 transcript variants (TV) on the levels and subcellular localization of PS1 and other γ-secretase complex components and subsequent γ-secretase function in human embryonic kidney 293, human neuroblastoma SH-SY5Y, and mouse primary cortical cells. Full-length ubiquilin-1 TV1 and TV3 that lacks the proteasome-interaction domain, increased full-length PS1 levels as well as induced accumulation of high-molecular-weight PS1 and aggresome formation. Accumulated PS1 co-localized with TV1 or TV3 in the aggresomes. Electron microscopy indicated that aggresomes containing TV1 or TV3 were targeted to autophagosomes. TV1- and TV3-expressing cells did not accumulate other unrelated proteasome substrates, suggesting that the increase in PS1 levels was not due to a general impairment of the ubiquitin-proteasome system. Furthermore, PS1 accumulation and aggresome formation coincided with alterations in Aβ levels particularly in cells over-expressing TV3. These effects were not related to altered γ-secretase activity or PS1 binding to TV3. Collectively, our results indicate that specific ubiquilin-1 TVs can cause PS1 accumulation and aggresome formation, which may impact AD pathogenesis or susceptibility.

Keywords

proteasomal degradation; β-amyloid precursor protein; PEN-2; transcript variant; high-molecular-weight forms

[§]Correspondence: Dr. Mikko Hiltunen Institute of Clinical Medicine - Neurology University of Eastern Finland P.O. Box 1627 70211 Kuopio Finland Tel. +358 40 3552014 Fax. +358 17 162048 mikko.hiltunen@uef.fi.
[*]These authors contributed equally.

INTRODUCTION

Alzheimer's disease (AD) is the most common neurodegenerative disorder characterized by the decline of cognitive functions and memory impairment. Typical neuropathological features of AD include amyloid plaques, formed by β-amyloid (Aβ) peptides, neurofibrillary tangles (NFTs), consisting of hyperphosphorylated microtubule-associated protein tau, and global synapse loss in cortical brain areas. While NFTs are formed as a result of imbalanced function of protein kinases and phosphatases, Aβ is produced by sequential proteolytic processing of β-amyloid precursor protein (APP) by β- and γ-secretases (1). Presenilin (PS) is one of the key players in AD pathogenesis. Mutations in *PSEN1* or *PSEN2* genes that encode for PS1 or PS2, respectively, cause the familial, early-onset form of AD, and result in increased Aβ generation and Aβ42:Aβ40 ratio (2). Moreover, PS is the catalytically active component of γ-secretase, an enzymatic complex that also contains nicastrin (NCT), APH1, and PEN-2 (3–6).

Ubiquilin-1 is a protein that has been shown to interact with and stabilize PS (7–9). We have previously shown that ubiquilin-1, both genetically and functionally, associates with AD (10–12). The ubiquilin-1 gene (*UBQLN1)* allelic variant UBQ8i is associated with an increased risk for AD, via altering *UBQLN1* alternative splicing. This resulted in the increased generation of the ubiquilin-1 transcript variant 2 (TV2) lacking exon 8 as compared to the full-length TV1 in AD brain (10). Down-regulation of ubiquilin-1 in cells altered the maturation and processing of APP and resulted in increased Aβ production (11). Furthermore, ubiquilin-1 has been shown to co-localize with NFTs in AD and Lewy bodies in Parkinson's disease brain, implying that it may affect the pathogenesis of neurodegenerative diseases beyond AD (7). Ubiquilin-1 contains an N-terminal ubiquitin-like (UBL) domain, which mediates its interaction with the 19S regulatory subunit of the 26S proteasome complex, and a C-terminal ubiquitin-associated (UBA) domain, which preferentially binds poly-ubiquitinated proteins (13). Since ubiquilin-1 regulates proteasomal degradation of various proteins, including cyclin A, γ-aminobutyric acid receptor, hepatitis C virus RNA-dependent RNA polymerase, and PS (7,14–16), it has been suggested that ubiquilin-1 acts as a shuttle between proteins destined for degradation and the ubiquitin-proteasome system (UPS) (17,18).

To date, four alternatively spliced ubiquilin-1 TVs (TV1–TV4) have been identified in human brain (10,19; see Figure 1A). Endoplasmic reticulum (ER) stress is a condition when unfolded proteins strongly accumulate in cells. We recently showed that under tunicamycin-induced ER stress, TV1, TV2, and most prominently TV3, which almost completely lacks the UBL domain, alleviated the induction of pro-apoptotic C/EBP homologous protein (CHOP) and increased cell viability. TV4, the shortest variant, had no effect. These data suggest that specific ubiquilin-1 TVs may confer cytoprotection under stress (19). Furthermore, UBL and UBA domains have recently proven important for ubiquilin-1 function in aggresome formation and targeting of aggregated proteins to autophagosomes (20–22). Aggresomes are cytoplasmic inclusions formed when the amount of aggregated, misfolded proteins overwhelms the protein refolding chaperone system and the UPS. The accumulated proteins are transported on the microtubuli to the perinuclear region and surrounded by vimentin filaments to form the aggresome, which may then be discarded from the cells by autophagy (23,24). The current data suggest that a cytoprotective role for ubiquilin-1 by targeting proteins either to proteasomal degradation or to the aggresomes, during abnormal protein accumulation in different stress conditions or neurodegenerative diseases. In the present study, we provide evidence that specific ubiquilin-1 TVs are involved in both PS1 accumulation and in targeting proteins to the aggresomes.

RESULTS

Co-expression of PS1 and ubiquilin-1 TV3 results in the accumulation of high-molecular-weight PS1 forms

Previous studies have provided controversial data regarding the effects of ubiquilin-1 on the levels of PS1 and other γ-secretase complex components (8,11). Furthermore, due to the fact that ubiquilin-1 transcript variants are expressed in the brain tissue of both AD patients and control subjects in a possibly altered ratio (10,19), it is important to assess the functional relevance of these variants in the key molecular pathways in AD pathogenesis. To characterize the effects of the four known ubiquilin-1 variants (TV1, TV2, TV3, and TV4) (19) on the expression levels of PS1, the TVs were transiently over-expressed with PS1 in HEK293-AP-APP cells, which over-express alkaline phosphatase-conjugated APP. Figure 1A depicts the structures of the TVs, showing exons encoding the different domains, including the N-terminal UBL and the C-terminal UBA domain. Each of the TVs and PS1 were robustly over-expressed, although TV3 expression was consistently slightly lower than that of the other TVs (Figure 1B). Most interestingly, TV3, but not the other TVs, appeared to prominently induce formation of high-molecular weight (HMW) PS1 forms, as indicated by the smear above the full-length PS1 (PS1-FL) band in the Western blot (Figure 1B).

We next investigated whether the different TVs affected the levels of individual γ-secretase complex components. Transient transfection of HEK293-AP-APP cells led to an average ~3-fold over-expression of TV1 and TV2 (GAPDH normalized TV1 levels = 310 ± 46 %, $p< 0.01$ and TV2 levels = 299 ± 25 %, $p<0.01$ when compared to the levels of GAPDH normalized endogenous TV1 in the control samples = 100 ± 7.4 %) (Figure 2A). Since the endogenous levels of TV3 and TV4 were undetectable in the control samples (Figure 2B), the ratio of TV3 levels to those of the endogenous TV1 (= 0.6 ± 0.1) and the ratio of TV4 levels to the endogenous TV1 levels (= 2.0 ± 0.8) were determined from the TV3 and TV4 transfected samples to verify the over-expression status of these variants. Over-expression of TV1 or TV2 resulted in a significant increase in the full-length PS1 and PS1 C-terminal fragment (PS1-CTF) levels as compared to control cells (Figure 2A). On the other hand, over-expression of TV4 did not significantly affect the levels of PS1-CTF, but lowered the levels of PS1 N-terminal fragment (PS1-NTF). Over-expression of TV3 again induced HMWPS1 formation (Figure 2B). All four TVs caused a significant increase in PEN-2 levels, but had no effect on the levels of APH1aL or NCT. Also, PEN-2 levels positively correlated with PS1-CTF levels (Supplement figure 1A), but not with the levels of APH1aL (Supplement figure 1B).

Since γ-secretase is the enzyme complex cleaving APP to produce Aβ, we measured Aβ and total secreted APP (sAPPtot) levels in the culture media of the HEK293-AP-APP cells over-expressing different ubiquilin-1 TVs (GAPDH normalized TV1 levels = 268 ± 56 %, $p<0.01$ and TV2 levels = 282 ± 42 %, $p<0.01$ when compared to GAPDH normalized endogenous TV1 levels in the control samples = 100 ± 21 %. TV3/TV1 ratio = 0.6 ± 0.1 and TV4/TV1 ratio = 2.0 ± 0.8). TV1, TV2, and TV3 decreased the levels of Aβ40, Aβ42, and sAPPtot (= sAPPα + sAPPβ) in the culture media. TV3 displayed the most pronounced effect and all three parameters were significantly reduced in TV3-expressing cells (Figure 2C).

To assess whether the decreased Aβ levels resulted from an altered γ-secretase activity, we performed γ-secretase activity measurements in HEK293-AP-APP cells co-transfected with PS1 and TV1, TV3 or control plasmids (Figure 2D). The over-expression status of TV1 and TV3 was determined from the cytosolic protein fraction (GAPDH normalized TV1 levels = 489 ± 95 % when compared to GAPDH normalized endogenous TV1 levels in the control samples = 100 ± 21 %, $p<0.01$. TV3/TV1 ratio = 1.1 ± 0.4). There were no differences with respect to γ-secretase activity between control and TV1 or TV3 over-expressing samples.

Samples treated with the γ-secretase inhibitor L685,458 revealed on average a 60 % reduction in γ-secretase activity, similar to that seen previously (25; data not shown). Overall, these data suggest that ubiquilin-1 TVs differentially modulate γ-secretase complex component levels as well as Aβ and sAPPtot secretion without affecting the γ-secretase activity.

Over-expression of ubiquilin-1 TV3, but not TV1, stabilizes full-length PS1, without causing general impairment of the UPS

The formation of HMW-PS1 in cells over-expressing TV3 suggested that PS1 accumulated in these cells. To investigate whether PS1 accumulation was due to alteration in PS1 half-life, cycloheximide time course was performed in HEK293-AP-APP cells over-expressing PS1 and TV1 or TV3 (GAPDH normalized TV1 levels = 583 ± 251 % when compared to GAPDH normalized endogenous levels of TV1 in the control samples = 100 % at time point 0 hours, $p<0.001$. TV3/TV1 ratio = 0.7 ± 0.3 at time point 0 hours). Cycloheximide inhibits *de novo* protein synthesis and thus degradation of existing proteins can be followed over time. Western blot analysis at 0, 1, 2, 4, and 8 hours of cycloheximide treatment once again demonstrated the presence of HMW-PS1 in cells over-expressing PS1 and TV3 (Figure 3A). Assessment of PS1 turnover revealed that the half-life of full-length PS1 was not significantly different between cells over-expressing PS1 with TV1 (2.8 ± 0.8 hours) and control (4.1 ± 0.7 hours) (Figure 3A and B). In the presence of TV3, however, the half-life of full-length PS1 (6.4 ± 1.4 hours) was significantly increased when compared to cells over-expressing PS1 with TV1 ($p = 0.017$). Moreover, TV3 over-expressing cells showed a trend towards a significant increase in the half-life of full-length PS1 when compared to control cells ($p = 0.06$). Consistent with previous results (7, 26), PS1-CTF, PS1-NTF and ubiquilin-1 levels remained stable in all cells through 8 hours. Collectively, these data suggest that ubiquilin-1 TV3 stabilizes full-length PS1 leading to an increased half-life and PS1 accumulation.

To examine the subcellular localization of the different TVs, we created tagged myc-TV1-mRFP or myc-TV3-mRFP expression vectors (Figure 4A). Western blot analysis was performed to confirm that myc-TV1-mRFP and myc-TV3-mRFP functionally acted in the same way as their wild-type counterparts in HEK293-AP-APP cells. Most importantly, HMW-PS1 was formed in cells transfected with myc-TV3-mRFP, but not myc-TV1-mRFP (Figure 4B, middle panel). In addition, TV3, but not TV1, containing only the N-terminal myc tag (myc-TV3 and myc-TV1, respectively; Supplement figure 2A), induced HMW-PS1 formation in the same way as the wild-type TV3 and the myc-TV3-mRFP in HEK293-APAPP cells (Supplement figure 2B). These experiments confirmed that the tags did not interfere with the induction of HMW-PS1 formation by TV3.

In order to elucidate the mechanism underlying TV3-induced PS1 accumulation, we investigated whether it resulted from a general impairment of the UPS. For this purpose, HEK293T cells stably expressing the Ub^{G76V}-YFP reporter UPS substrate were co-transfected with mRFP (control), myc-TV1-mRFP, or myc-TV3-mRFP and PS1. In these reporter cells, increased YFP fluorescence would indicate UPS impairment. Over-expression of myc-TV3-mRFP was once more confirmed to cause HMW-PS1 formation in HEK293T Ub^{G76V}-YFP cells (Figure 5A). The YFP intensities were not increased in cells over-expressing myc-TV1-mRFP or myc-TV3-mRFP, indicating that the UPS was not grossly impaired (Figure 5B–D, top panels, and 5E). Treatment with the proteasomal inhibitor MG132 expectedly led to a dramatic, but similar increase in the YFP fluorescence in all the transfected cells (Figure 5B–D, bottom panels, and 5E). Altogether, these data demonstrate that TV3-induced accumulation of HMW-PS1 does not result from a global UPS impairment.

Co-expression of PS1 with ubiquilin-1 TV1 or TV3 enhances aggresome formation

We then performed a thorough investigation of HEK293-AP-APP cells co-over-expressing PS1 with mRFP control plasmid, myc-TV1-mRFP, or myc-TV3-mRFP by wide-field fluorescence and confocal laser scanning microscopy to assess whether the accumulated HMW-PS1 could be visualized. PS1 showed a normal cellular distribution in mRFP-transfected control cells and it localized in intracellular structures resembling the endoplasmic reticulum (ER) and Golgi and on or close to the plasma membrane as assessed by both wide-field fluorescence and confocal microscopy (Figures 6A and 8A). Both myc-TV1-mRFP and myc-TV3-mRFP highly co-localized with PS1 in intracellular compartments and on the plasma membrane. There was no apparent difference in the PS1 subcellular localization or co-localization with myc-TV1-mRFP or myc-TV3-mRFP (Figures 6B and C, 8A, and data not shown). However, cells co-expressing PS1 and myc-TV1-mRFP (Figure 6B) or PS1 and myc-TV3-mRFP (Figures 6C and 8A) appeared to contain cytoplasmic aggresome-like inclusions more often than the control cells (Figure 6A). PS1 and myc-TV1-mRFP or myc-TV3-mRFP strongly co-localized in these inclusions (Figures 6B and C). Quantification indicated that ~42% of the cells co-expressing PS1 and myc-TV3-mRFP and ~22% of the cells co-expressing PS1 with myc-TV1-mRFP contained aggresomes as compared to ~11% in mRFP control cells (Figure 6D). High-throughput fluorescence lifetime monitoring assay revealed that there was no statistically significant difference between PS1 and TV1 or TV3 proximity (lifetime) or proportion of interacting molecules (Table 1), indicating that there was no difference between PS1 interaction with TV1 and TV3. These data suggest that the enhanced aggresome formation in TV3-over-expressing cells is not related to altered PS1 binding to TV3.

Western blotting and microscopy of HEK-293-AP-APP cells transiently transfected with myc-TV1-mRFP or myc-TV3-mRFP and endogenously expressing PS1 did not reveal the presence of HMW-PS1 or aggresomes (data not shown). The same was true for H4 human neuroglioma cells stably over-expressing TV1 or TV3 (19) with endogenous PS1 expression (data not shown). These data suggest that over-expression of ubiquilin-1 TVs alone does not result in the formation of aggresomes, but a specific interaction with an accumulating protein, such as PS1, is required. This further supports the previously suggested role for ubiquilin-1 as a shuttle protein between accumulated proteins and the UPS. The present observations also demonstrate that PS1 co-over-expression with especially TV3 in HEK293-AP-APP cells is a useful cell-based model to study aggresome formation. This is well in accordance with previous data in HEK cells showing PS1 accumulation in the aggresomes under proteasomal inhibition (27).

The intermediate filament protein vimentin is known to redistribute to aggresomes and form a cage surrounding the core of aggregated proteins (23,27). In mRFP control cells, vimentin was ubiquitously present with a strong localization near the plasma membrane (Figures 7A and 8B). In contrast, vimentin robustly redistributed to PS1- and myc-TV1-mRFP or myc-TV3-mRFP containing aggresomes (Figures 7B and C, and 8B). Moreover, confocal microscopy revealed that vimentin was reorganized to surround the myc-TV1-mRFP or myc-TV3-mRFP -positive aggresomal core, agreeing with previous reports (Figure 8B and data not shown; 23,27,28). Although vimentin drastically redistributed in aggresome-containing cells, the overall cell morphology was similar to the cells not containing aggresomes as estimated visually. Quantification of the cells having aggresomes with relocated vimentin showed that ~40% of the cells co-expressing PS1 with myc-TV3-mRFP and ~24 % of the cells co-expressing PS1 and myc-TV1-mRFP contained aggresomes compared to ~12% in control cells (Figure 7D). These numbers are highly similar to those obtained in the quantification of aggresome-containing cells on the basis of PS1 and myc-TV1-mRFP or myc-TV3-mRFP co-localization (Figure 6D).

Aggresomes typically co-localize with γ-tubulin, a marker protein of the microtubule-organizing center (MTOC) where protein aggregates are actively transported to (23,27,28). γ-tubulin-positive MTOC co-localized within the aggresomes in cells co-expressing PS1 and myc-TV3-mRFP (Figure 9A). Furthermore, confocal analysis confirmed the subcellular co-localization of PS1, myc-TV3-mRFP, and γ-tubulin, in the aggresomes (Figure 9B). Collectively, these data suggest that formation of aggresomes containing PS1 and myc-TV1-mRFP or myc-TV3-mRFP was significantly enhanced in HEK293-AP-APP cells.

We next examined if aggresomes were formed in primary cortical cells from transgenic mice over-expressing APP and PS1 with the familial ΔE9 mutation (lacking exon 9). Western blotting did not indicate the presence of HMW-PS1 in cortical cells transfected with either myc-TV1 or myc-TV3 (Figure 10A). Interestingly, we found a significant increase in the Aβ40 levels in the media of both myc-TV1 and myc-TV3 over-expressing cells (GAPDH normalized myc-TV1 levels = 251 ± 73 % when compared to GAPDH normalized endogenous TV1 levels in the control samples = 100 %, $p<0.01$. myc-TV3/endogenous TV1 ratio = 0.7 ± 0.1), and a significant increase in Aβ42 levels in only myc-TV1 over-expressing cells (Figure 10B), opposite to the observations in HEK293-AP-APP cells. However, microscopy of the primary neurons revealed the presence of aggresome-like inclusions in neurons over-expressing myc-TV1-mRFP and myc-TV3-mRFP. These neuronal aggresomes contained both PS1 and myc-TV1-mRFP or myc-TV3-mRFP and caused a typical indentation of the nucleus similarly to the aggresomes in HEK293-AP-APP cells (Figures 10C and D). Moreover, vimentin robustly redistributed to these aggresomes, confirming that the neuronal cytoplasmic inclusions indeed were aggresomes (Supplement figure 3). Formation of PS1-containing aggresomes was not observed in neurons transfected with the control plasmid (Figures 10C and D). Interestingly, astrocytes, which contained barely detectable levels of PS1, did not have aggresomes, and myc-TV1-mRFP or myc-TV3-mRFP were evenly localized in the cytoplasm (data not shown). According to microscopy, more astrocytes than neurons were successfully transfected with myc-TV1-mRFP and myc-TV3-mRFP. As astrocytes were proven not to contain aggresomes, low transfection efficiency in neurons could explain why HMW-PS1 was not detected in the Western blot (Figure 10A). Nevertheless, these data indicate that both TV1- and TV3 -over-expression leads to PS1 accumulation in aggresomes in PS1ΔE9-over-expressing neurons in a similar manner to HEK293-APAPP cells.

We also investigated aggresome formation in human SH-SY5Y neuroblastoma cells over-expressing APP751 isoform (SH-SY5Y-APP751), which is a commonly used neuronal cell line in elucidating AD-related molecular mechanisms (29,30). The cells were co-transfected with PS1 and mRFP, myc-TV1-mRFP, or myc-TV3-mRFP and examined by fluorescence microscopy. In a similar manner to HEK-293-AP-APP cells and primary cortical neurons, aggresomes were commonly observed in SH-SY5Y-APP751 cells co-expressing PS1 with TV1 or TV3. Furthermore, PS1 strongly co-localized with TV1 or TV3 in the aggresomes (Supplement figure 4B and C). Quantification demonstrated a significant increase in the aggresome formation in SH-SY5Y-APP751 cells co-expressing PS1 with TV3 (~25%) as compared to the control cells co-expressing PS1 and the mRFP control plasmid (~16%). The number of SH-SY5Y-APP751 cells co-expressing PS1 and TV1 and having aggresomes (~21%) was also significantly higher than the number in the control cells (Supplement figure 4D). Interestingly, aggresome formation was not observed in H4 human neuroglioma cells, which are cells of glial origin, co-expressing PS1 and myc-TV1-mRFP or myc-TV3-mRFP (data not shown). However, these data agree well with our present findings and imply that neuronal cells may efficiently utilize the aggresome pathway under conditions of protein accumulation in contrast to glial cells. Overall, the fact that aggresomes were formed in neurons and neuron-like cells in addition to HEK cells, but not in glial cells, implicate that there may be cell type-specific differences in the propensity to form aggresomes.

Electron microscopy confirms the presence of ubiquilin-1 TV1 and TV3 in aggresomes and autophagosomes

At the electron microscopical level, cells transfected with myc-TV3-mRFP or myc-TV1-mRPF and PS1 were found to contain large electron dense amorphous aggregates having characteristics of aggresomes (Figures 11A, 11D–F). These aggregates were either freely dispersed in the cytoplasm or enclosed in the double-membrane vacuoles, also known as autophagosomes. The cells contained a high number of mitochondria that were accumulated especially in the perinuclear area facing towards the indentation of the nucleus. The cells also contained a high number of autophagic vacuoles, secondary lysosomes containing partially destructed cellular material as well as late lysosomes having accumulated unidentified electron dense material. In general, autophagic vacuoles were of the highest prevalence compared to other vacuoles belonging to the lysosomal pathway. Typical for these cells was that they also contained large multilamellarmultivesicular inclusions (Figure 11B). These were composed of double-membranes wrapping several times around one or more cores. The interior of these inclusions were filled by electron dense membranous structures, vacuoles containing material of different electron density, and small vesicles as well as cytoplasm having normal appearance. Occasionally, inclusions were composed of double membrane segments (smooth endoplasmic reticulum) that formed a concentric large cluster without a clearly identifiable core (Figure 11C). Nevertheless, also found in these inclusions were electron dense vacuoles accumulated in the central region. Bundles of intermediate filaments could occasionally be identified in the neighbourhood of the inclusion bodies (Figure 11C) or free aggresomes (Figure 11F). TV3 appeared to induce more pronounced changes in the cells than TV1.

Using photoconversion of mRFP fluorescent signal to electron dense DAB-deposits, we found that mRFP was typically located in between the double-membranes that formed autophagic vacuoles (Figure 11A). These vacuoles were found to engulf aggresomes or cytoplasm. DAB-deposits were occasionally found also inside and in association with cisternas of the endoplasmic reticulum. Near the nucleus, electron dense deposits were located inside the multilamellarmultivesicular inclusions (Figure 11B and 11C). Immunogold staining for myc revealed that myc is highly concentrated in free cytoplasmic aggregates (Figure 11D and 11E). Relatively strong labeling was also seen in the aggresome-like aggregates that were wrapped inside the autophagosomes. Immunolabeling of late lysosomes in the multilamellar-multivesicular inclusions was less pronounced. Taken together, these data confirm the light microscopical data that TV1 and TV3 localize within aggresomes and further indicate that aggresomes or other cytoplasmic aggregates containing TV1 or TV3 may be targeted to autophagosomes.

DISCUSSION

Ubiquilin-1 is known to co-localize and interact with PS1 and PS2 at least partially via its UBA domain (7–9,11,31). Ubiquilin-1 was also reported to specifically promote PS2 accumulation without affecting PS2 half-life in HeLa cells and to modulate PS1 and PS2 NTF and CTF levels as well as those of PEN-2 and NCT (7,8). Our previous studies, in contrast, indicated unaltered γ-secretase component levels and activity after ubiquilin-1 knock-down in H4 and HEK293 cells (11). Here we found that individual ubiquilin-1 TVs differentially affected the levels of full-length PS1, PS1-NTF and PS1-CTF, and other γ-secretase components as well as secretion of Aβ and sAPP in HEK293 APAPP cells. Nonetheless, it should be emphasized that the effects on γ-secretase component levels were moderate and the most striking findings were the formation of HMW-PS1 specifically in cells over-expressing TV3 and the accumulation of PS1 in the aggresomes in both TV1- and TV3-over-expressing HEK293 AP-APP cells. In addition, Aβ and/or sAPPtot secretion significantly decreased in these cells, which agree with our previous data showing that TV1

knockdown in HEK293-AP-APP cells increased Aβ and sAPPtot secretion due to altered APP trafficking (11). Furthermore, our present γ-secretase activity measurements in HEK293 AP-APP cells showed no differences between control and TV1- or TV3-over-expressing cells, providing additional evidence that altered Aβ and sAPPtot secretion is not due to changes in γ-secretase activity, but rather may relate to altered trafficking of APP in HEK293-AP-APP cells as previously shown in this cell line (11). In contrast to HEK293-AP-APP cells, we observed that secreted Aβ levels were increased after TV1 and TV3 over-expression in the primary cortical cultures, which was accompanied with formation of aggresomes in neurons, but not in astrocytes. This finding again is in line with the previous ubiquilin-1 TV1 over-expression data in SH-SY5Y neuroblastoma cells showing increased levels of AICD and sAPPα (32). Collectively, these results emphasize the cell type-specific differences in terms of APP metabolism, processing and Aβ production upon ubiquilin-1 over-expression. They also indicate that the accumulation of PS1 in the aggresomes *per se* does not affect the γ-secretase activity. It is possible, however, that while the PS1 dependent γ-secretase activity is unaltered, PS1 accumulation and aggresome formation could affect other PS1-related cellular functions.

Over-expression of ubiquilin-1 has been shown to decrease the ubiquitination and degradation of PS2 and HMW-PS2, and to result in the formation of PS2- and ubiquilin-1-containing aggresomes (7,33). Our data showing that HMW-PS1 and aggresome formation were significantly augmented, especially in cells co-over-expressing TV3 and PS1, is in agreement with these findings. Mounting evidence indicates that ubiquilin-1 mediates the degradation of poly-ubiquitinated proteins, such as PS1, by targeting them to the proteasome, thus creating a link between the proteins destined for degradation and the UPS (13,17,18). TV3, which lacks most of the UBL domain, most profoundly increased the formation of PS1-containing aggresomes. Since PS1 interaction with TV1 was comparable to its interaction with TV3, it is unlikely that increased aggresome formation would be a result of a more pronounced PS1 binding to TV3 as compared to TV1. Thus, our data suggest that TV3 may be incapable of efficiently delivering PS1 to the proteasome, which results in PS1 accumulation in the aggresomes. In accordance with previous reports (7), aggresome formation was also significantly increased in cells over-expressing TV1 and PS1. On the other hand, over-expression of TV1 or TV3 alone did not result in the formation of aggresomes, and a specific interaction with an accumulating protein, PS1 in this case, was required. These notions together provide further support for the previously suggested role for ubiquilin-1 as a shuttle protein between accumulated proteins and the UPS. Furthermore, aggresomes were formed in 10–15% of PS1-over-expressing control cells depending on the cell line, suggesting that accumulated PS1 is targeted to the aggresomes and that the presence of TV1 or TV3 augments this phenomenon. Aggresomes were also found in primary cortical neurons and neuronal SHSY5Y cells over-expressing PS1 and TV1 or TV3, suggesting that ubiquilin-1-induced aggresome formation is not limited only to HEK cells. The fact that aggresomes were not observed in primary astrocytes or H4 glial cells after PS1 and ubiquilin-1 over-expression may indicate that different cell types may differ in their propensity to use the aggresome pathway for discarding accumulated proteins. According to current hypothesis, aggresome formation is a cytoprotective response to neutralize potentially harmful protein aggregates and to facilitate their disposal by autophagy (23,34). Consistent with this idea, our data suggest that aggresomes and other cytoplasmic aggregates containing TV1 or TV3 are targeted to autophagosomes, which may ultimately lead to autolysosomal protein degradation.

PS1 has been shown to form HMW complexes and to accumulate in aggresomes in response to proteasomal inhibition or heat shock (27,35). We found no evidence for a general UPS impairment in UPS reporter cells over-expressing TV3 or TV1. These findings rule out UPS dysfunction as a mechanism behind PS1 accumulation and aggresome formation. Rather,

our data suggest that TV3 stabilizes full-length PS1 leading to an increased half-life and subsequent PS1 accumulation, because TV3 is unable to efficiently deliver PS1 for proteasomal degradation (36;Figure 12). Furthermore, HMW-PS1 forms are likely resistant to proteasomal degradation and thus accumulate in the aggresomes. These data imply that HMW-PS1 consists mainly of full-length PS1 and that especially accumulated full-length PS1 is targeted to the aggresomes. Endogenously expressed full-length PS1 is not typically detected in the Western blots due to its extensive endoproteolysis (26). Therefore, it is likely that HMW-PS1 accumulation and aggresome formation were not observed in the cells over-expressing TV1 or TV3 with endogenous PS1 expression, as the levels of full-length PS1 remained low.

Ubiquilin-1 also targets other neurodegenerative disease-associated proteins to aggresomes and autophagosomes (21,37). Ubiquilin-1 UBL domain was necessary for aggresome formation in a poly-glutamine disease model, where ubiquilin-1 binding to epidermal growth factor substrate 15 (EPS15), an endocytic protein, was enhanced, subsequently promoting the transport of aggregated proteins to the aggresomes (20). We found that TV3, which has been shown to be expressed in the AD brain (19), and which lacks the majority of the UBL domain, most profoundly enhanced the formation of PS1-containing aggresomes. However, the remaining N-terminal portion of the UBL domain in TV3 may enable EPS15 binding and aggresome formation. In addition, ubiquilin-1 potentiates the aggregation of and co-aggregates with TDP-43 (43-kDa TAR DNA-binding domain protein), a protein present in ubiquitin-positive cytoplasmic neuronal aggregates in fronto-temporal dementia and amyotrophic lateral sclerosis. Ubiquilin-1 UBA domain mediated the interaction with poly-ubiquitinated TDP-43 and was required for TDP-43 aggregation and autophagosomal targeting (21). Interestingly, the AD-associated ubiquilin-1 variant lacking the exon 8 failed to efficiently recruit TDP-43 to the cytosolic aggregates (21). Ubiquilin-1 or 2 also associate with autophagosomes and other autophagy-destined protein aggregates via UBA domains, such as aggregated Huntington's disease (HD)-associated huntingtin. This interaction was required for cell survival during nutrient starvation (22). Furthermore, ubiquilin-1 interacts with mTOR (mammalian target of rapamycin), a central inhibitor of autophagy. Inhibition of mTOR induces autophagy and reduces the toxicity of poly-glutamine expansions *in vivo* in HD (38,39). Taken together, increasing evidence implicates ubiquilin-1 in the proteasomal degradation and accumulation or aggregation of proteins associated with different neurodegenerative diseases. Our data show that specific ubiquilin-1 TVs regulate the degradation and accumulation of AD-associated PS1. Therefore, ubiquilin-1 alternative splicing, which also takes place in the human brain, may be an important factor determining whether ubiquilin-1 prevents or promotes neurodegeneration.

MATERIALS AND METHODS

cDNA constructs

Plasmids containing ubiquilin-1 TV1 (full-length), TV2 (lacking exon 8), TV3 (lacking exons 2–4), TV4 (lacking exons 4–11) and wild-type PS1 cDNAs were used in transfections. TV1 and TV3 cDNA constructs containing either a myc tag at the 5'-end (yielding N-terminally myc-tagged TVs) or both 5'-myc tag and a monomeric red fluorescent protein (mRFP) tag at the 3'-end (yielding TVs with N-terminal myc and C-terminal mRFP tag) were also used. The myc tag adds ~3 kDa and myc together with mRFP add ~39 kDa to the molecular weight of the TVs. pcDNA3.1, HIV or mRFP plasmids were used as controls. The myc-tagged and the myc- and mRFP-tagged constructs were created as follows: the open reading frames of TV1 and TV3 were PCR-amplified from cDNA while introducing *Sal*I and *Nhe*I-STOP codon-*Kpn*I restriction sites flanking the 5' and 3' ends of the open reading frame, respectively. The PCR products were inserted in frame into pCMV-myc plasmid (Invitrogen) using *Sal*I and *Kpn*I restriction sites creating myc-TV1 and myc-

TV3. Myc-TV1 and myc-TV3 were excised with *Apa*I and *Nhe*I and inserted in a mRFP expression vector resulting in myc-TV1-mRFP and myc-TV3-mRFP. The following primers were used: Ubiquilin-1 sense primer TCGGTCGACg **ATG** GCC GAG AGT GGT GAA AGC and ubiquilin-1 antisense primer CGCGGTACC **CTA** gacc ggt GAT GGC TGG GAG CCC AGT AAC (underlined, restriction sites; bold, start and stop codons).

Cell culture and transfection

Human embryonic kidney (HEK) 293 cells stably over-expressing alkaline phosphatase-conjugated amyloid precursor protein (AP-APP) were cultured in Dulbecco's modified Eagle's medium (DMEM) containing 10% fetal bovine serum (FBS), 2 mM L-glutamine, 100 U/ml penicillin, and 100 μg/ml streptomycin (DMEM-C) and supplemented with 50 μg/ml hygromycin B and 0.3 μg/ml puromycin in a humidified cell culture incubator in 5% CO_2 atmosphere (40). Human neuroblastoma SHSY5Y cells stably over-expressing the APP751 isoform and human neuroglioma H4 cells stably over-expressing ubiquilin-1 TV1 or TV3 were cultured as previously described (19,29). Cell culture reagents were from Gibco or Invitrogen. HEK293-AP-APP, SHSY5Y, and H4 cells were reverse-transfected using Lipofectamine Reagent (Invitrogen) according to the manufacturer's instructions. Briefly, the cDNA-Lipofectamine complexes were mixed with the cells in a tube and the cells were then plated on poly-D-lysine-coated (PDL; 100 μg/ml; Sigma) 6-well plates (Nunc) at the density of ~350000 cells/well and allowed to transfect overnight. The cells were used in the experiments 48 hours after transfection.

UPS reporter cell experiments

HEK293T cells were stably transfected with an expression plasmid encoding the reporter substrate ubiquitin^{G76V}-yellow fluorescent protein (Ub^{G76V}-YFP) (41) and cultured in DMEM supplemented with 10% FBS, 10 U/ml penicillin, 10 μg/ml streptomycin, and 400 μg/ml G418. Cells were transiently transfected by electroporation with expression plasmids encoding myc-TV1-mRFP, myc-TV3-mRFP, or mRFP and plated on glass coverslips coated with polyethyleneimine. After 24 hours, cells were washed, fixed with 4 % paraformaldehyde (PFA) in PBS and mounted in Mowiol (Mowiol 40–88, glycerol, Tris pH 8.5, DABCO). Cells were analysed with a wide-field fluorescence microscope (Leica DMI 6000B) provided with Hamamatsu C10600-10B (ORCA-R2) camera and X-Cite exacte mercury lamp. Images were quantified using Volocity Quantitation software (Improvision). YFP fluorescence was quantified in mRFP-positive cells, which were defined as objects with a minimal object size of 50 μm^2 and a minimal mRFP intensity of 300 AU.

Primary cortical cell culture and transfection

Primary cortical cells were harvested from embryonic day 18 transgenic mouse embryos over-expressing human APP containing the Swedish double mutation (K595N/M596L) and human PS1ΔE9 (deletion of exon 9) mutant as previously described (42). Cells were plated (200000/well) on PDL-coated 12-well plates or coverslips in DMEM-C. Following cell attachment (3 hours after plating), the medium was replaced with serum-free Neurobasal medium supplemented with 1 × B27 and 2 mM L-glutamine (Gibco, Invitrogen). Half of the medium was refreshed every fourth day. The cells were allowed to mature for 12 days before transfection with NeuroMag (OZ Biosciences, France). The cultures contained approximately 95% neurons and 5% glia at the time of transfection. NeuroMag transfections were performed according to manufacturer's protocol. Briefly, half of the medium was changed 24 hours before transfection. cDNAs (2 μg) were diluted in Neurobasal medium and mixed with NeuroMag transfection reagent. NeuroMag/cDNA complexes were incubated for 20 min before adding to the cells. Cell plates were placed on a magnetic plate in the incubator for 15 min to allow cell magnetofection. The cells were cultured for 48 hours before analyses.

Western blot analysis

Total protein lysates were prepared using TPER tissue extraction buffer (Pierce) supplemented with a protease inhibitor mixture (Thermo Scientific) and centrifugation at 10000 × *g* for 10 min. Protein concentrations were determined using BCA protein assay kit (Pierce). Proteins (20–50 μg) were separated on 4–12% Bis-Tris gels (Invitrogen) under reducing conditions and blotted onto polyvinylidene difluoride (Amersham Hybond-P, GE Healthcare) membranes. Blots were probed with the following antibodies: mouse anti-ubiquilin-1 (detects the epitope in the middle of ubiquilin-1, 35–4400, 1:1000, Zymed Laboratories Inc.) and rabbit anti-ubiquilin-1 (detects the 2–18 epitope in the N-terminal part of ubiquilin-1, 1:1000, Calbiochem) to detect ubiquilin-1 TVs, mouse anti-PS1 recognizing the PS1 loop region (MAB5232, 1:1000, Chemicon) to detect full-length PS1 (PS1-FL) and PS1-CTF, rabbit anti-PS1 (Ab14; 1:1000, a gift from Dr. Samuel E. Gandy) for detecting PS1-FL and PS1 N-terminal fragment (NTF), and mouse anti-glyceraldehyde-3-phosphate dehydrogenase (GAPDH; ab8245, 1:15000, Abcam) or mouse anti-β-tubulin (1:1000, Sigma) for controlling equal loading and for normalization of the protein levels in each sample. After incubation with appropriate horse radish peroxidase (HRP)-conjugated secondary antibodies (GE Healthcare), proteins were detected by using enhanced chemiluminescence substrate (ECL, Amersham Biosciences, GE Healthcare) and ImageQuant RT ECL Imager (GE Healthcare). Images were quantified using Quantity One software (Bio-Rad).

Cycloheximide time course

HEK293-AP-APP cells were reverse-transfected using Lipofectamine Reagent (Invitrogen) with TV1 + PS1, TV3 + PS1, or control plasmid + PS1. Transfected cells were split into five wells representing 0, 1, 2, 4, and 8 hour time points for cycloheximide time course. Cycloheximide was added to transfected cells at 30 μg/ml concentration and incubated with the cells for 0, 1, 2, 4, and 8 hours. Thirty μg of total protein from each time point was used for Western blotting. The full-length PS1 (PS1-FL) levels at each time point were normalized to the PS1-FL level at 0 hours and plotted against hours of cycloheximide treatment to obtain the half-life of PS1-FL. The half-life of PS1-FL was calculated by plotting intensity values (normalized to the PS1-FL/GAPDH value at 0 h) with respect to chase time. Linear fitting was subsequently performed to obtain half-life calculations.

Secreted APP and Aβ measurements

Total sAPP (sAPPtot) and Aβ levels were measured from HEK293-AP-APP cell culture media as described previously (11). Briefly, aliquots of conditioned media were heat-inactivated at 65°C for 30 min after which 20 μl of the conditioned medium was added to 200 μl of reaction solution with 5 mg of p-nitrophenyl phosphate (Sigma) as a substrate. Absorbance was read at 405 nm. Each experiment was carried out in triplicate. Aβ x-40 and x-42 levels (pg/ml) were quantified from HEK293-AP-APP culture media using sandwich ELISA and normalized to total protein levels (mg) (43). Each experiment was carried out at least in triplicate. Aβ x-40 and x-42 levels (pg/ml) from primary cortical culture media were measured from 50 μl of sample using an ELISA assay kit and normalized to total protein levels (mg) (The Genetics Company, Switzerland).

γ-secretase activity assay

γ-secretase activity measurements were performed from CHAPSO-solubilized HEK293-AP-APP cell membranes as previously described (25). Briefly, membrane fractions from HEK293-AP-APP cells transfected with PS1 and TV1, TV3 or pcDNA3.1 plasmids were isolated by homogenizing cells with a 25 gauge needle 10 times in buffer B [20 mM HEPES pH 7.5, 150 mM KCl, 2 mM EGTA + protease inhibitor mixture (Thermo Scientific)]

followed by centrifugation in 100000 × *g* for 1 hour at +4°C. Supernatants were applied to Western blot analysis to confirm TV1 and TV3 over-expression status. Membrane pellets were washed with buffer B, centrifuged 100000 × *g* for 30 minutes, re-suspended in buffer B + 1% CHAPSO, and finally centrifuged at 100000 × *g* for 30 minutes. Equal amounts of CHAPSO-solubilized membrane lysates (124 μg) were incubated overnight at 37°C in 150 μl of substrate buffer (50 mM Tris-HCl pH 6.8, 2 mM EDTA, 0.25% CHAPSO) with 8 μM substrate peptide. Samples treated with 100 μM γ-secretase inhibitor L685,458 or DMSO were used to validate the specificity of the γ-secretase activity assay. Samples were briefly centrifuged and supernatants were transferred to a 96-well plate. Fluorescence was measured using Wallac 1420 Victor™ Multilabel Counter (PerkinElmer) plate reader with excitation wavelength of 355nm and emission wavelength of 460nm.

Immunofluorescence and confocal microscopy

Cells were fixed in 4% PFA or ice-cold acetone-methanol solution (1:1; for γ-tubulin staining). The cells were permeabilized and unspecific antibody binding was blocked by a 30-min incubation in phosphate-buffered saline (PBS; DPBS, Lonza) containing 0.1% Triton X-100 and 5% bovine serum albumin (BSA; fraction V, Sigma). Primary antibodies were incubated with the cells for 1.5 hours at the following dilutions: mouse anti-PS1 (MAB 5232, Chemicon) 1:400; mouse anti-vimentin (RV202, BD Pharmingen) 1:50; and rabbit anti-γ-tubulin (ab11317, Abcam) 1:5000, followed by one-hour incubation with secondary Alexa Fluor® 488 goat anti-mouse (1:500, Molecular Probes), Alexa Fluor® 488 goat anti-rabbit (1:300, Molecular Probes), or goat anti-rabbit Cy5 (1:1000, Jackson ImmunoResearch Laboratories) antibody. The nuclei were stained with Hoechst 33342 (1:5000; Sigma). Staining without primary antibodies was used as a negative control. Wide-field images were taken with Olympus BX40-FLA fluorescence microscope at 40X magnification. Single optical z-sections were obtained with Nikon Eclipse-TE300 microscope and Ultra VIEW laser scanning confocal unit (Perkin Elmer) at 60× magnification. Photomicrographs were processed by using Adobe Photoshop software (Adobe Systems, San Jose, CA, USA)

Stereological quantification of aggresomes

Quantification of the number of cells containing aggresomes was performed stereologically under a Nikon Eclipse E600 fluorescence microscope at 40× magnification using the StereoInvestigator 2000 program (MicroBrightField, Inc., Colchester, VA). Aggresomes in cells over-expressing myc-TV1-mRFP or myc-TV3-mRFP (red) and positive for PS1 or redistributed vimentin (green) and containing concave nuclei at the site of aggresomes were scored positive out of the total number of myc-TV1-mRFP or myc-TV3-mRFP over-expressing cells. Altogether, ≥1000 HEK293-AP-APP cells or ≥650 SH-SY5Y-APP751 cells were counted/sample from three independent transfections. Data are shown as % of cells with aggresomes/total number of cells ± standard deviation (SD).

Electron microscopy

DAB-photoconversion—To visualize mRFP at the electron microscopic level, the photoconversion method described by Meißlitzer-Ruppitsch et al. was used (44) Briefly, HEK293-AP-APP cells were fixed in 4% PFA for 30 min, washed in 0.05 M Tris buffer, pH 7.4, and preincubated in 0.1% 3,3'-diaminobenzidine (DAB) (D5637, Sigma) for 30 min. Photoconversion was carried out under mercury lamp (100 W Ushio USH102D) until the fluorescence had faded. Thereafter, the cells were treated with a solution containing 1% OsO4 (19130, EMS) and 1.5% potassium ferrocyanide (K4(Fe(CN)6) × 3H20, Merck) for 15 min followed by incubation in 1% OsO4. Cells were then processed for transmission electron microscopy as previously described (45). Briefly, the dehydration and embedding procedure was done *in situ* on the original cell culture dishes. The beam capsules filled with

LX-112 were laid upside-down on the dishes and polymerized at 60°C for 48 hours. Ultrathin sections were cut on copper and nickel grids.

Immunogold staining—Sections mounted on nickel grids were used for postembedding immunogold staining for myc. Sections were first treated with 1% periodic acid (30325, Riedel-de Haen) in ddH2O (10 min) followed by incubation in 3% sodium periodate (10259, BDH) in ddH2O (2 × 30 min). To reduce unspecific binding, sections were first incubated in 0.05 M glycine (33226, Sigma) in PBS and then in PBS containing 5% BSA (A-2153, Sigma) and 0.1% cold water fish gelatine (G-7041, Sigma). After washing in 0.1% BSA-c (B2518, Sigma) in PBS (2 × 5 min), sections were incubated in mouse anti-myc (1:100, 05-724, Upstate) overnight in a humid chamber. Sections were then washed in BSA-c-PBS (6 × 5 min) followed by incubation in 15 nm gold-conjugated anti-mouse (1:30, GAM, 815.022, Aurion) for 2 hours. The antibody dilutions were made in 0.1% BSA-c-PBS containing 0.5% Tween 20 (93773, Sigma). After immunogold staining, sections were washed in BSA-c-PBS (6 × 5 min) and PBS (2 × 5 min), and then fixed for 5 min in 2% glutaraldehyde (16220, EMS) and washed in ddH2O (5 min). Both the sections on copper and nickel grids were stained with uranyl acetate (02624-A, SPI-Chem) for 30 min and lead citrate (Ultrastain solution 2, 70553022, Leica) for 2 min. The sections were examined and photographed at Jeol 1200 EX electron microscope.

Fluorescence Lifetime Imaging Microscopy

The interaction between PS1 and ubiquilin-1 TV1 and TV3 transcript variants in intact cells was analyzed using TECAN FLT Ultraevolution system (Tecan Trading AG, Switzerland) as described previously (9,11). Briefly, CHO cells co-expressing wild-type PS1 and V5-tagged ubiquilin-1 TV1 and TV3 were double-immunostained with Cy3 and Alexa430 fluorescently labeled anti-PS1 C-terminus (CT) and anti-V5 antibodies, respectively. Forster resonance energy transfer (FRET) between the donor (Alexa 430) and acceptor (Cy3) fluorophores was assessed in a high-throughput screen format. The donor fluorophore lifetime and FRET strength were monitored as measures of a relative proximity between the PS1 CT and ubiquilin-1-V5 (TV1 and TV3) and as a proportion of interacting molecules in each sample, respectively (9,11).

Statistical Analyses

Statistical analyses were performed using SPSS program, version 14.0. Independent samples t-test, Mann-Whitney U-test or one-way analysis of variance (ANOVA) was used to test statistical significance between sample groups. Values are indicated as mean ± standard deviation (SD). The level of statistical significance was set to $p < 0.05$.

Supplementary Material

Refer to Web version on PubMed Central for supplementary material.

Acknowledgments

This study was supported by EC FP6, MEST-CT-2005-019217 (to JV), the Health Research Council of the Academy of Finland (to AH, HS, and MH), EVO grant 5772708 of Kuopio University Hospital (to HS), the Nordic Centre of Excellence in Neurodegeneration (to NPD, HS, and MH), Sigrid Juselius Foundation (to MH), the Swedish Research Council (to NPD), the Wenner-Gren Foundation (to CB), NIH AG15379 grant (to OB), and “Cure Alzheimer's Fund” and NIA (to RT). The authors wish to thank Dr. Stefan Lichtenthaler (Adolf-Butenandt-Institute, Ludwig-Maximilians-University, Munich, Germany) for the generous gift of the HEK293-AP-APP cells, Dr. Samuel E. Gandy (Mount Sinai School of Medicine, New York, NY) for kindly providing the Ab14 antibody, and Dr. Garry Wong (A.I.Virtanen Institute for Molecular Sciences, University of Eastern Finland) for revising the language of the manuscript.

REFERENCES

1. Selkoe DJ. Cell biology of protein misfolding: The examples of Alzheimer's and Parkinson's diseases. Nature Cell Biology 2004;6:1054–1061.
2. Tanzi RE, Bertram L. Twenty years of the Alzheimer's disease amyloid hypothesis: A genetic perspective. Cell 2005;120:545–555. [PubMed: 15734686]
3. Francis R, McGrath G, Zhang J, Ruddy DA, Sym M, Apfeld J, Nicoll M, Maxwell M, Hai B, Ellis MC, Parks AL, Xu W, Li J, Gurney M, Myers RL, Himes CS, Hiebsch R, Ruble C, Nye JS, Curtis D. Aph-1 and pen-2 are required for notch pathway signaling, gamma-secretase cleavage of betaAPP, and presenilin protein accumulation. Developmental Cell 2002;3:85–97. [PubMed: 12110170]
4. Goutte C, Tsunozaki M, Hale VA, Priess JR. APH-1 is a multipass membrane protein essential for the notch signaling pathway in caenorhabditis elegans embryos. Proceedings of the National Academy of Sciences of the United States of America 2002;99:775–779. [PubMed: 11792846]
5. Yu G, Nishimura M, Arawaka S, Levitan D, Zhang L, Tandon A, Song YQ, Rogaeva E, Chen F, Kawarai T, Supala A, Levesque L, Yu H, Yang DS, Holmes E, Milman P, Liang Y, Zhang DM, Xu DH, Sato C, Rogaev E, Smith M, Janus C, Zhang Y, Aebersold R, Farrer LS, Sorbi S, Bruni A, Fraser P, St George-Hyslop P. Nicastrin modulates presenilin-mediated notch/glp-1 signal transduction and betaAPP processing. Nature 2000;407:48–54. [PubMed: 10993067]
6. Edbauer D, Winkler E, Regula JT, Pesold B, Steiner H, Haass C. Reconstitution of gamma-secretase activity. Nature Cell Biology 2003;5:486–488.
7. Mah AL, Perry G, Smith MA, Monteiro MJ. Identification of ubiquilin, a novel presenilin interactor that increases presenilin protein accumulation. The Journal of Cell Biology 2000;151:847–862. [PubMed: 11076969]
8. Massey LK, Mah AL, Monteiro MJ. Ubiquilin regulates presenilin endoproteolysis and modulates gamma-secretase components, pen-2 and nicastrin. The Biochemical Journal 2005;391:513–525. [PubMed: 15975090]
9. Thomas AV, Herl L, Spoelgen R, Hiltunen M, Jones PB, Tanzi RE, Hyman BT, Berezovska O. Interaction between presenilin 1 and ubiquilin 1 as detected by fluorescence lifetime imaging microscopy and a high-throughput fluorescent plate reader. The Journal of Biological Chemistry 2006;281:26400–26407. [PubMed: 16815845]
10. Bertram L, Hiltunen M, Parkinson M, Ingelsson M, Lange C, Ramasamy K, Mullin K, Menon R, Sampson AJ, Hsiao MY, Elliott KJ, Velicelebi G, Moscarillo T, Hyman BT, Wagner SL, Becker KD, Blacker D, Tanzi RE. Family-based association between Alzheimer's disease and variants in UBQLN1. The New England Journal of Medicine 2005;352:884–894. [PubMed: 15745979]
11. Hiltunen M, Lu A, Thomas AV, Romano DM, Kim M, Jones PB, Xie Z, Kounnas MZ, Wagner SL, Berezovska O, Hyman BT, Tesco G, Bertram L, Tanzi RE. Ubiquilin 1 modulates amyloid precursor protein trafficking and abeta secretion. The Journal of Biological Chemistry 2006;281:32240–32253. [PubMed: 16945923]
12. Li A, Xie Z, Dong Y, McKay KM, McKee ML, Tanzi RE. Isolation and characterization of the drosophila ubiquilin ortholog dUbqln: In vivo interaction with early-onset Alzheimer disease genes. Human Molecular Genetics 2007;16:2626–2639. [PubMed: 17704509]
13. Ko HS, Uehara T, Tsuruma K, Nomura Y. Ubiquilin interacts with ubiquitylated proteins and proteasome through its ubiquitin-associated and ubiquitin-like domains. FEBS Letters 2004;566:110–114. [PubMed: 15147878]
14. Funakoshi M, Geley S, Hunt T, Nishimoto T, Kobayashi H. Identification of XDRP1; a xenopus protein related to yeast Dsk2p binds to the N-terminus of cyclin A and inhibits its degradation. The EMBO Journal 1999;18:5009–5018. [PubMed: 10487753]
15. Bedford FK, Kittler JT, Muller E, Thomas P, Uren JM, Merlo D, Wisden W, Triller A, Smart TG, Moss SJ. GABA(A) receptor cell surface number and subunit stability are regulated by the ubiquitin-like protein plic-1. Nature Neuroscience 2001;4:908–916.
16. Gao L, Tu H, Shi ST, Lee KJ, Asanaka M, Hwang SB, Lai MM. Interaction with a ubiquitin-like protein enhances the ubiquitination and degradation of hepatitis C virus RNA-dependent RNA polymerase. Journal of Virology 2003;77:4149–4159. [PubMed: 12634373]

17. Kleijnen MF, Shih AH, Zhou P, Kumar S, Soccio RE, Kedersha NL, Gill G, Howley PM. The hPLIC proteins may provide a link between the ubiquitination machinery and the proteasome. Molecular Cell 2000;6:409–419. [PubMed: 10983987]

18. Kleijnen MF, Alarcon RM, Howley PM. The ubiquitin-associated domain of hPLIC-2 interacts with the proteasome. Molecular Biology of the Cell 2003;14:3868–3875. [PubMed: 12972570]

19. Lu A, Hiltunen M, Romano DM, Soininen H, Hyman BT, Bertram L, Tanzi RE. Effects of ubiquilin 1 on the unfolded protein response. Journal of Molecular Neuroscience : MN 2009;38:19–30. [PubMed: 18953672]

20. Heir R, Ablasou C, Dumontier E, Elliott M, Fagotto-Kaufmann C, Bedford FK. The UBL domain of PLIC-1 regulates aggresome formation. EMBO Reports 2006;7:1252–1258. [PubMed: 17082820]

21. Kim SH, Shi Y, Hanson KA, Williams LM, Sakasai R, Bowler MJ, Tibbetts RS. Potentiation of amyotrophic lateral sclerosis (ALS)-associated TDP-43 aggregation by the proteasome-targeting factor, ubiquilin 1. The Journal of Biological Chemistry 2009;284:8083–8092. [PubMed: 19112176]

22. N'Diaye EN, Kajihara KK, Hsieh I, Morisaki H, Debnath J, Brown EJ. PLIC proteins or ubiquilins regulate autophagy-dependent cell survival during nutrient starvation. EMBO Reports 2009;10:173–179. [PubMed: 19148225]

23. Kopito RR. Aggresomes, inclusion bodies and protein aggregation. Trends in Cell Biology 2000;10:524–530. [PubMed: 11121744]

24. Olzmann JA, Li L, Chin LS. Aggresome formation and neurodegenerative diseases: Therapeutic implications. Current Medicinal Chemistry 2008;15:47–60. [PubMed: 18220762]

25. Farmery MR, Tjernberg LO, Pursglove SE, Bergman A, Winblad B, Naslund J. Partial purification and characterization of gamma-secretase from post-mortem human brain. The Journal of Biological Chemistry 2003;278:24277–24284. [PubMed: 12697771]

26. Ratovitski T, Slunt HH, Thinakaran G, Price DL, Sisodia SS, Borchelt DR. Endoproteolytic processing and stabilization of wild-type and mutant presenilin. The Journal of Biological Chemistry 1997;272:24536–24541. [PubMed: 9305918]

27. Johnston JA, Ward CL, Kopito RR. Aggresomes: A cellular response to misfolded proteins. The Journal of Cell Biology 1998;143:1883–1898. [PubMed: 9864362]

28. Namekata K, Nishimura N, Kimura H. Presenilin-binding protein forms aggresomes in monkey kidney COS-7 cells. Journal of Neurochemistry 2002;82:819–827. [PubMed: 12358787]

29. Sarajarvi T, Haapasalo A, Viswanathan J, Makinen P, Laitinen M, Soininen H, Hiltunen M. Down-regulation of seladin-1 increases BACE1 levels and activity through enhanced GGA3 depletion during apoptosis. The Journal of Biological Chemistry 2009;284:34433–34443. [PubMed: 19815556]

30. Kuhn PH, Wang H, Dislich B, Colombo A, Zeitschel U, Ellwart JW, Kremmer E, Rossner S, Lichtenthaler SF. ADAM10 is the physiologically relevant, constitutive alpha-secretase of the amyloid precursor protein in primary neurons. The EMBO Journal. 2010

31. Ford DL, Monteiro MJ. Studies of the role of ubiquitination in the interaction of ubiquilin with the loop and carboxyl terminal regions of presenilin-2. Biochemistry 2007;46:8827–8837. [PubMed: 17614368]

32. Zhang C, Khandelwal PJ, Chakraborty R, Cuellar TL, Sarangi S, Patel SA, Cosentino CP, O'Connor M, Lee JC, Tanzi RE, Saunders AJ. An AICD-based functional screen to identify APP metabolism regulators. Molecular Neurodegeneration 2007;2:15. [PubMed: 17718916]

33. Massey LK, Mah AL, Ford DL, Miller J, Liang J, Doong H, Monteiro MJ. Overexpression of ubiquilin decreases ubiquitination and degradation of presenilin proteins. Journal of Alzheimer's Disease: JAD 2004;6:79–92.

34. Jaeger PA, Wyss-Coray T. All-you-can-eat: Autophagy in neurodegeneration and neuroprotection. Molecular Neurodegeneration 2009;4:16. [PubMed: 19348680]

35. Kovacs I, Lentini KM, Ingano LM, Kovacs DM. Presenilin 1 forms aggresomal deposits in response to heat shock. Journal of Molecular Neuroscience: MN 2006;29:9–19. [PubMed: 16757805]

36. Matiuhin Y, Kirkpatrick DS, Ziv I, Kim W, Dakshinamurthy A, Kleifeld O, Gygi SP, Reis N, Glickman MH. Extraproteasomal Rpn10 restricts access of the polyubiquitin-binding protein Dsk2 to proteasome. Molecular Cell 2008;32:415–425. [PubMed: 18995839]

37. Doi H, Mitsui K, Kurosawa M, Machida Y, Kuroiwa Y, Nukina N. Identification of ubiquitin-interacting proteins in purified polyglutamine aggregates. FEBS Letters 2004;571:171–176. [PubMed: 15280037]

38. Wu S, Mikhailov A, Kallo-Hosein H, Hara K, Yonezawa K, Avruch J. Characterization of ubiquilin 1, an mTOR-interacting protein. Biochimica Et Biophysica Acta 2002;1542:41–56. [PubMed: 11853878]

39. Ravikumar B, Vacher C, Berger Z, Davies JE, Luo S, Oroz LG, Scaravilli F, Easton DF, Duden R, O'Kane CJ, Rubinsztein DC. Inhibition of mTOR induces autophagy and reduces toxicity of polyglutamine expansions in fly and mouse models of huntington disease. Nature Genetics 2004;36:585–595. [PubMed: 15146184]

40. Lichtenthaler SF, Dominguez DI, Westmeyer GG, Reiss K, Haass C, Saftig P, De Strooper B, Seed B. The cell adhesion protein P-selectin glycoprotein ligand-1 is a substrate for the aspartyl protease BACE1. The Journal of Biological Chemistry 2003;278:48713–48719. [PubMed: 14507929]

41. Menendez-Benito V, Verhoef LG, Masucci MG, Dantuma NP. Endoplasmic reticulum stress compromises the ubiquitin-proteasome system. Human Molecular Genetics 2005;14:2787–2799. [PubMed: 16103128]

42. Smith IF, Hitt B, Green KN, Oddo S, LaFerla FM. Enhanced caffeine-induced Ca2+ release in the 3xTg-AD mouse model of Alzheimer's disease. Journal of Neurochemistry 2005;94:1711–1718. [PubMed: 16156741]

43. Wolfe MS, Xia W, Ostaszewski BL, Diehl TS, Kimberly WT, Selkoe DJ. Two transmembrane aspartates in presenilin-1 required for presenilin endoproteolysis and gamma-secretase activity. Nature 1999;398:513–517. [PubMed: 10206644]

44. Meiblitzer-Ruppitsch C, Vetterlein M, Stangl H, Maier S, Neumuller J, Freissmuth M, Pavelka M, Ellinger A. Electron microscopic visualization of fluorescent signals in cellular compartments and organelles by means of DAB-photoconversion. Histochemistry and Cell Biology 2008;130:407–419. [PubMed: 18463889]

45. Miettinen R, Reunanen H. Vinblastine-induced autophagocytosis in cultured fibroblasts. Comparative Biochemistry and Physiology. C, Comparative Pharmacology and Toxicology 1991;99:29–34.

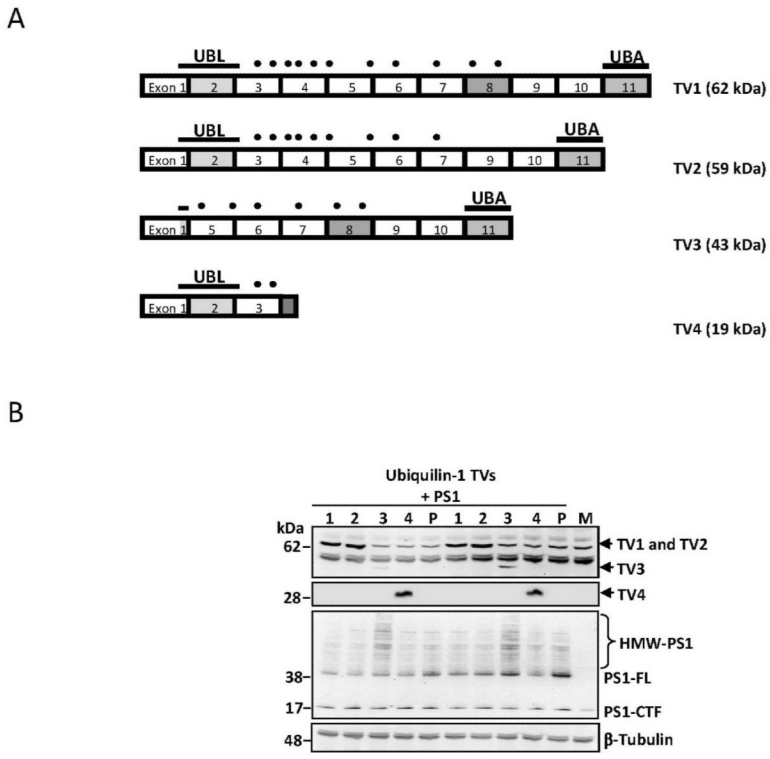

Figure 1. Co-expression of PS1 and ubiquilin-1 TV3 results in the accumulation of HMW-PS1 forms in HEK293-AP-APP cells

A) Schematic representation of the gene structure of *ubiquilin-1* transcript variants (TV1–4). Exons encoding the N-terminal ubiquitin-like (UBL) and the C-terminal ubiquitin-associated (UBA) domain are indicated. Black dots represent asparagineand proline-rich repeats that may mediate protein-protein interactions. *B)* Western blot showing the PS1 C-terminal fragment (PS1-CTF) and full-length PS1 (PS1-FL) levels in HEK293-AP-APP cells transiently co-expressing PS1 and different ubiquilin-1 TVs. Co-expression of PS1 and TV3 results in an increased accumulation of high-molecular weight PS1 (HMW-PS1). P, control plasmid; M, mock-transfection.

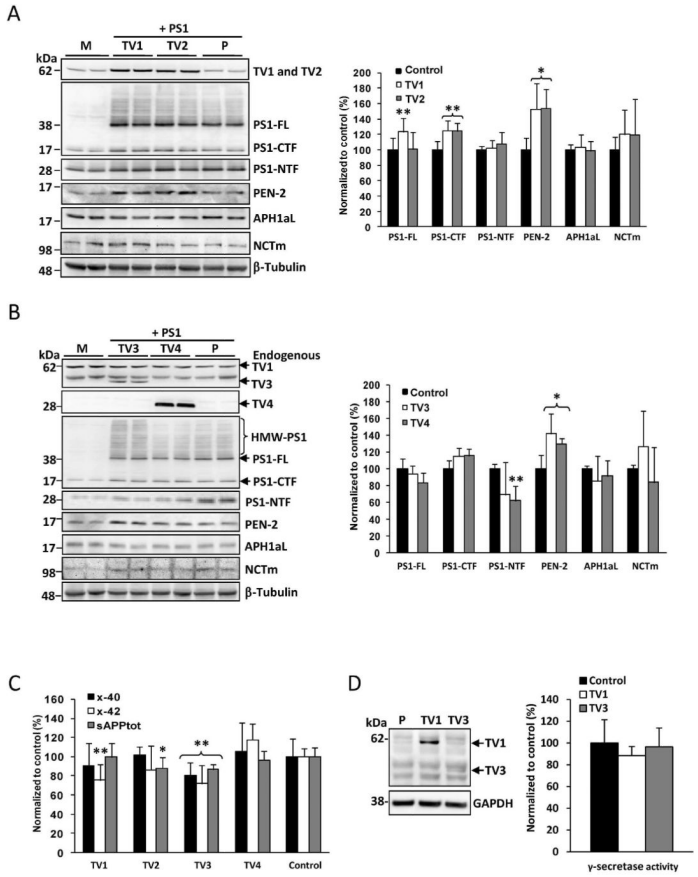

Figure 2. Co-expression of PS1 and ubiquilin-1 TVs increase PEN-2 levels and decrease Aβ40 and Aβ42 levels in HEK293-AP-APP cells

A, B) Western blots showing the levels of different γ-secretase complex components in HEK293-AP-APP cells co-expressing PS1 and ubiquilin-1 variants (TV1 and TV2 in *A*, TV3 and TV4 in *B*). β-tubulin-normalized PEN-2 levels are significantly increased in cells over-expressing ubiquilin-1 transcript variants, correlating with increased PS1-CTF levels. P, control plasmid; M, mock-transfection. *C)* Assessment of secreted Aβ40, Aβ42, and total sAPP (sAPPtot) levels from the culture media. Co-expression of PS1 and TV3 significantly reduce total protein-normalized Aβ40, Aβ42, and sAPPtot secretion. *D)* γ-secretase activity measurements in HEK293-APAPP cells co-transfected with PS1 and TV1, TV3, or control plasmid do not show differences between samples. TV1 and TV3 over-expression status was confirmed from the cytosolic protein fraction using Western blot analysis. Pearson's correlation coefficient test, $^{**}p < 0.01$, $^{*}p < 0.05$, $n \geq 3$, SD.

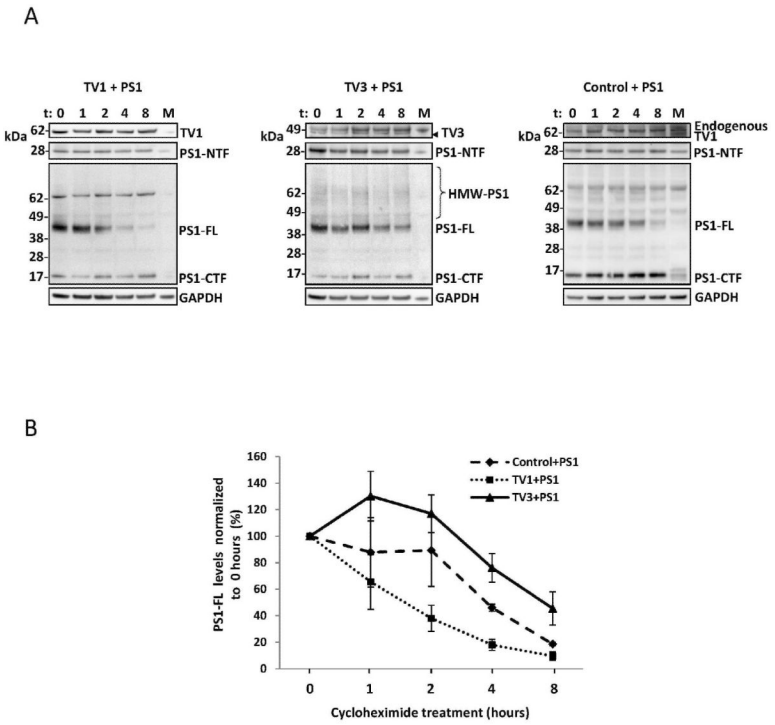

Figure 3. Over-expression of ubiquilin-1 TV1 or TV3 in HEK293-AP-APP cells affect full-length PS1 half-life differently

A) Western blot of cells co-over-expressing TV1, TV3 or control plasmid with PS1 and treated with cycloheximide (30 μg/ml) for 0, 1, 2, 4 and 8 hours. The HMW-PS1 forms start to accumulate after 2 hours in cells transfected with TV3. Concomitantly, the levels of full-length PS1 (PS1-FL) decrease. *B)* Quantification of the PS1-FL levels at different times after cycloheximide treatment. TV3 over-expression stabilizes the levels of PS1-FL as compared to TV1-over-expressing or control cells. SEM; M, mock-transfection; t, time (hours after treatment).

Figure 4. N- and C-terminally tagged ubiquilin-1 TV3, but not TV1, increases the accumulation of HMW-PS1 in HEK293-AP-APP cells

A) A schematic representation of the tagged myc-TV1-mRFP and myc-TV3-mRFP cDNA constructs. *B)* Western blot showing that co-expression of myc-TV3-mRFP with PS1 induced accumulation of HMW-PS1 in a similar manner to the untagged TV3 (shown in Figure 1A). P, control plasmid; mRFP, monomeric red fluorescent protein. *Asterisks* indicate degradation products of myc-TV1-mRFP and myc-TV3-mRFP.

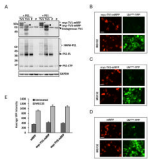

Figure 5. Over-expression of myc-TV1-mRFP or myc-TV3-mRFP does not result in a general UPS impairment in HEK293T Ub^{G76V}-YFP reporter cells

A) Western blot of Ub^{G76V}-YFP HEK293T cells over-expressing PS1-FL and myc-TV1-mRFP (*) or myc-TV3-mRFP (*arrow head*). Middle panel shows HMW-PS1 in myc-TV3-mRFP over-expressing cells. P, control plasmid. *B–D*) Micrographs of Ub^{G76V}-YFP HEK293T cells transiently transfected with myc-TV1-mRFP (*B*), myc-TV3-mRFP (*C*) or mRFP (control; *D*). Cells were either left untreated (top panels) or treated for 6 hrs with 10 μM proteasome inhibitor MG132 (bottom panels). Scale bar = 20μm. *E)* Quantification of YFP fluorescence in Ub^{G76V}-YFP HEK293T cells transiently transfected with myc-TV1-mRFP, myc-TV3-mRFP or mRFP. YFP fluorescence was quantified by selecting mRFP-positive objects using Volocity Quantitation software. Error bars represent standard error of mean (SEM) (n > 320 cells). There are no significant differences between YFP values of the mRFP-expressing cells (control) against myc-TV1-mRFP- or myc-TV3-mRFP-expressing cells (Student's *t*-test; untreated cells against MG132-treated cells). YFP, yellow fluorescent protein.

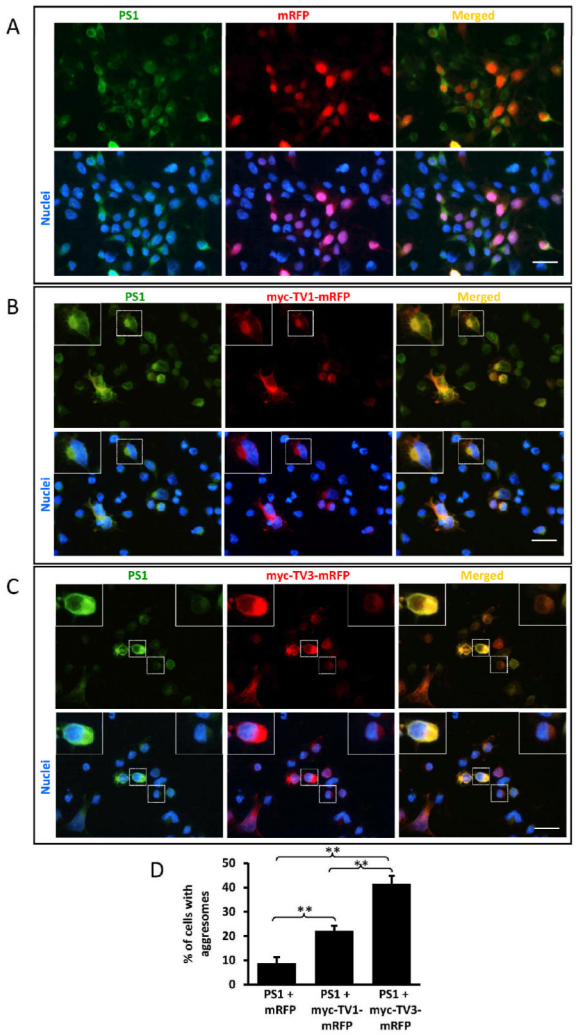

Figure 6. PS1 and ubiquilin-1 TV1 or TV3 co-localize in aggresomes in HEK293-AP-APP cells

A) Localization of PS1 in cells co-transfected with PS1 (*green*) and mRFP control plasmid (*red*). *B,C)* PS1 and TV1 or TV3 co-localize (*yellow*) in aggresomes in cells co-transfected with PS1 and myc-TV1-mRFP or myc-TV3-mRFP (*red*). Nuclei are shown in *blue*. Boxed individual cells containing an aggresome are shown at higher magnification in the insets. Wide-field fluorescence images were taken at 40× magnification. Scale bar = 20 μm for all images. *D)* Quantification of the number of cells containing TV1- or TV3- and PS1-positive aggresomes. Data are shown as % of cells with aggresomes/total number of cells ± SD, n = 3 (≥ 1000 cells), **p<0.001, One-way ANOVA, Newman-Keuls Multiple Comparison Test.

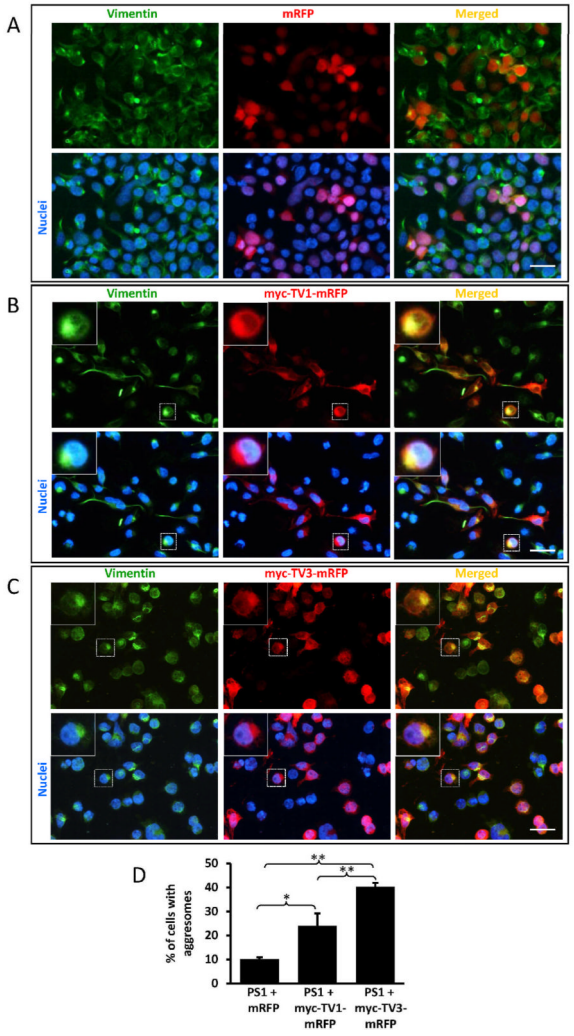

Figure 7. Vimentin redistributes to the aggresomes in HEK293-AP-APP cells co-transfected with PS1 and ubiquilin-1 TV1 or TV3

A) Normal distribution of vimentin (*green*) in cells co-transfected with PS1 and mRFP control plasmid (*red*). *B,C)* Vimentin redistributes to the aggresomes in cells co-transfected with PS1 and myc-TV1-mRFP or myc-TV3-mRFP (*red*). Co-localization is indicated by *yellow*. Nuclei are shown in *blue*. Boxed individual cells containing an aggresome are shown at higher magnification in the insets. Wide-field fluorescence images were taken at 40× magnification. Scale bar = 20 μm for all images. *D)* Quantification of the number of cells containing TV1- or TV3- and vimentin-positive aggresomes. Data are shown as % of cells with aggresomes/total number of cells ± SD, n = 3 (≥ 1000 cells), *p<0.01, **p<0.001 as indicated, One-way ANOVA, Newman-Keuls Multiple Comparison Test.

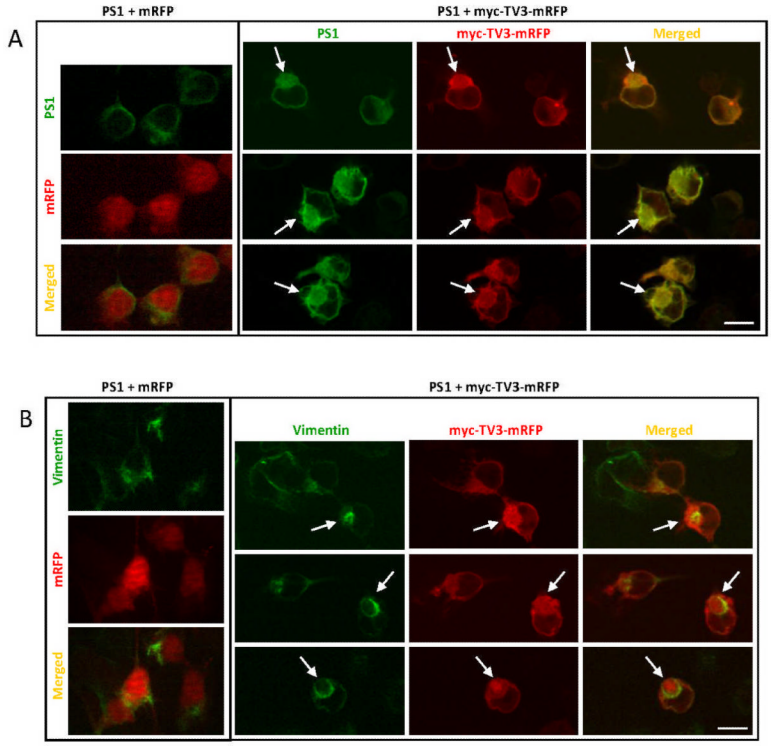

Figure 8. PS1 and ubiquilin-1 TV3 show similar subcellular distribution and co-localize in aggresomes, which are enveloped in a vimentin cage in HEK293-AP-APP cells

A) Subcellular localization of PS1 in cells co-transfected with PS1 (*green*) and mRFP control plasmid (left panel) or myc-TV3-mRFP (*red*; right panels). PS1 and TV3 co-localize (*yellow*) on the plasma membrane and in the aggresomes (*arrows*) in cells co-transfected with PS1 and myc-TV3-mRFP. *B)* Vimentin (*green*) localizes intracellularly and close to the plasma membrane in cells co-transfected with PS1 and mRFP control plasmid (left panel). In cells co-transfected with PS1 and myc-TV3-mRFP, vimentin redistributes to and forms an envelope around the aggresome, as indicated by a green ring surrounding the red TV3-containing aggresome core (right panels). Confocal microscope images show single optical z-sections taken at 60× magnification. Scale bar = 10 μm for all images.

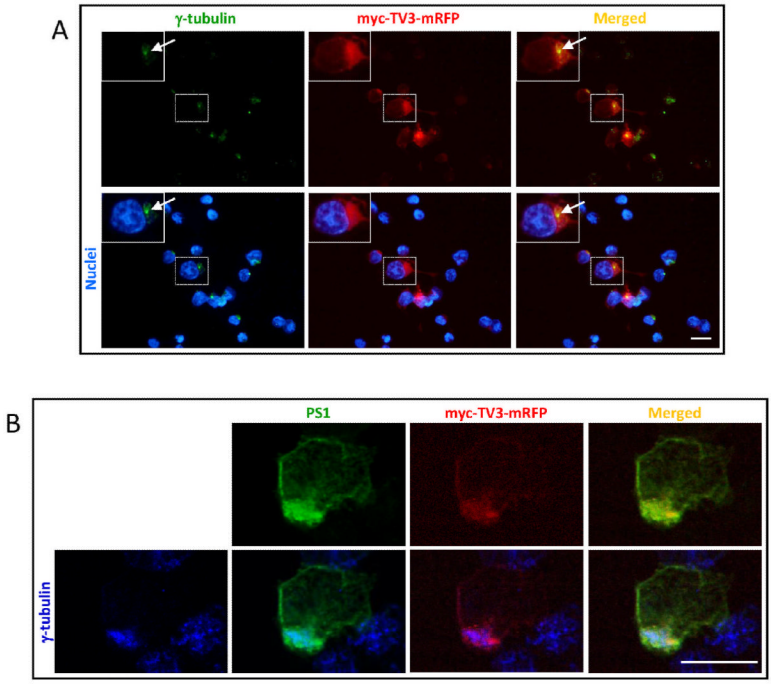

Figure 9. Aggresomes in HEK293-AP-APP cells co-expressing PS1 and ubiquilin-1 TV3 co-localize with γ-tubulin, a marker for the microtubule-organizing center

A) Aggresomes containing myc-TV3-mRFP (*red*) c o-localize with γ-tubulin (*green*) at the juxtanuclear microtubule-organizing center (MTOC). Co-localization is indicated by *yellow*. Nuclei are shown in *blue*. The boxed individual cell containing an aggresome is shown at higher magnification in the insets. *Arrow* points to the MTOC. Wide-field fluorescence images were taken at 40× magnification. Scale bar = 20 μm. *B)* Confocal microscope images of a cell co-transfected with PS1 and myc-TV3-mRFP confirming the co-localization of PS1 and myc-TV3-mRFP with γ-tubulin in the aggresome (*cyan blue* in merged image). Co-localization of PS1 and TV3 is indicated by *yellow*. Images show single optical z-sections taken at 60× magnification. Scale bar = 10 μm.

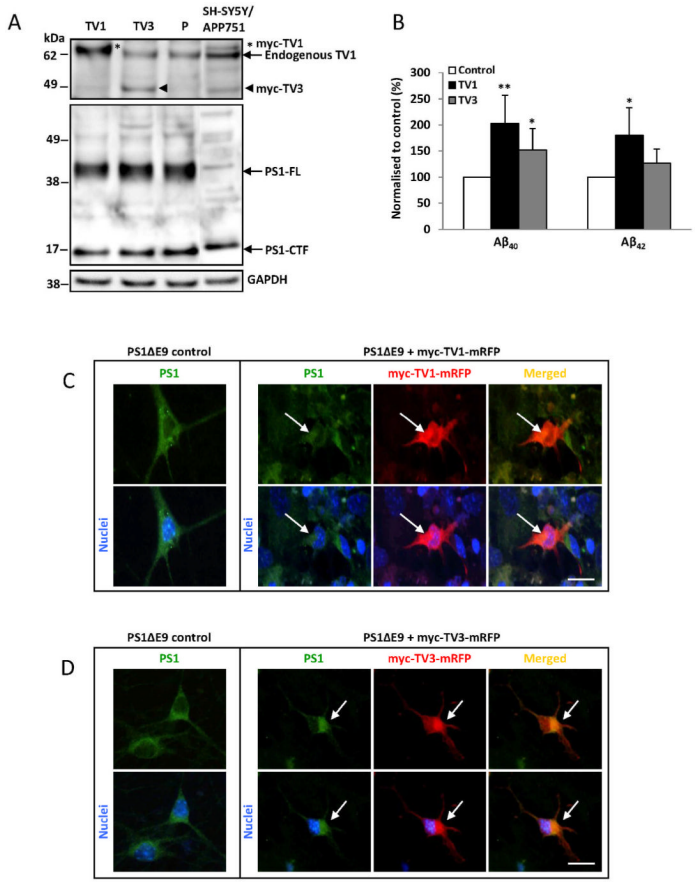

Figure 10. Aggresome formation in primary cortical cells of APP/PS1ΔE9 transgenic mice transfected with ubiquilin-1 TV1 or TV3

A) Western blot showing transient over-expression of myc-TV1 (251 ± 73 % when normalized to endogenous TV1 in control sample) and myc-TV3 (TV3 vs. endogenous TV1 ratio = 0.7 ± 0.1) in E18 cortical cultures from an APP/PS1ΔE9 transgenic mouse. The blot indicates PS1ΔE9 over-expression shown by the strong levels of PS1-FL. Staining with an antibody against PS1 did not demonstrate the presence of HMW-PS1 as in the case of HEK293-AP-APP cells over-expressing myc-TV3 (see Supplement figure 2). P, control plasmid. *B)* Total protein-normalized Aβ40 and Aβ42 measurements from the culture medium of APP/PS1ΔE9 primary cortical cells show a significant increase in Aβ40 levels in both myc-TV1 and myc-TV3 over-expressing cells. n=4, SD, *p<0.01, **p<0.005. C, D) PS1 co-localizes with TV1 or TV3 in the aggresomes in neurons from APP/PS1ΔE9 transgenic mice transfected with myc-TV1-mRFP or myc-TV3-mRFP. Left panels, control cortical neurons stained with PS1 antibody (*green*). Right panels, neurons transfected with myc-TV1-mRFP or myc-TV3-mRFP (*red*) containing an aggresome (*arrow*) next to the nucleus (*blue*). Co-localization is indicated by *yellow*. Wide-field fluorescence images were taken at 40× magnification. Scale bar = 10 μm for all images.

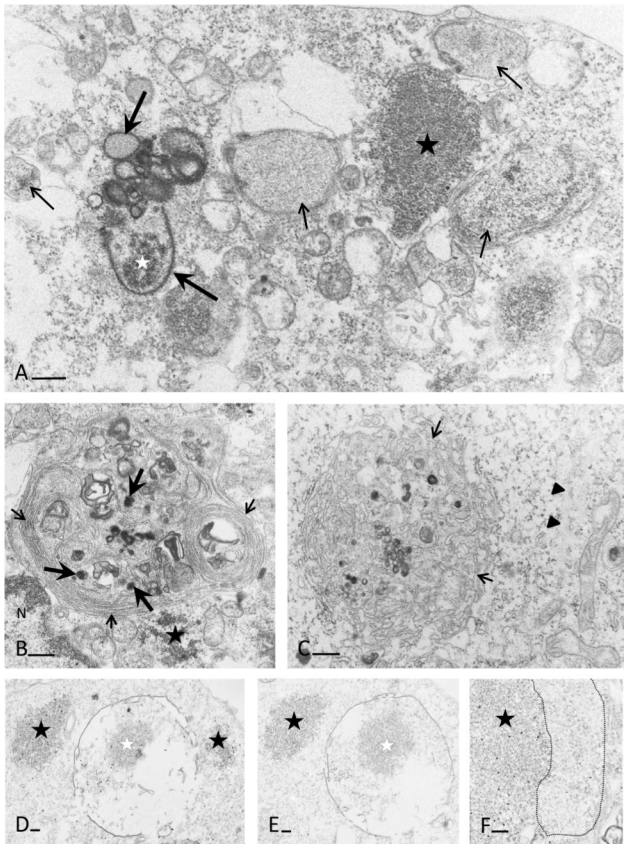

Figure 11. Ubiquilin-1 TV1 and TV3 localize in aggresomes and autophagosomes as revealed by electron microscopy

Electron micrographs of mRFP (*A–C*; scale 500 nm) and myc (*D–F*; scale 200 nm) localization in myc-TV3-mRFP and PS1 (*A, B, D, E, F*) and myc-TV1-mRFP and PS1 (*C*) transfected cells. *A)* Photoconversion of mRFP results in electron dense deposit formation that is located in between the double membranes forming autophagic vacuoles (*large arrows*). Aggregates are either freely dispersed in the cytoplasm (*black star*) or inside the forming autophagosome (*white star*). In general, autophagic vacuoles and lysosomes are numerous in myc-TV3-mRFP transfected cells (*thin arrows*). *B)* Large multilamellar-multivesicular inclusions are typically located near the indentation of the nucleus (N). Multiple layers of double membranes (*small arrows*) wrap around multivesicular bodies and vesicles many of which contain electron dense DAB-deposition (*thick arrows*). A free cytoplasmic aggresome (*black star*) is located near the inclusion body. *C)* As visualized in ultrathin electron microscopic section, short segments of endoplasmic reticulum (*small arrows*) form a multilamellar inclusion that contains electron dense vesicles. Thin intermediate filaments are seen in the neighbourhood (*arrowheads*). *D)* Gold particles are concentrated in the aggregates in a mycimmunostained section. Aggregates in the cytoplasm (*black arrows*) gather stronger immunoreactivity than that inside the vacuole (*white arrow*). *E)* Negative control section contains none or only a few gold particles. *F)* Higher magnification of an aggresome (*black star*) that contains multiple gold particles indicating myc-immunoreactivity. This aggresome has close contact with the neighbouring interfilament bundle (*dashed line around*). The fine structure of the filaments has suffered from etching of the resin that was required for the post-embedding immunostaining.

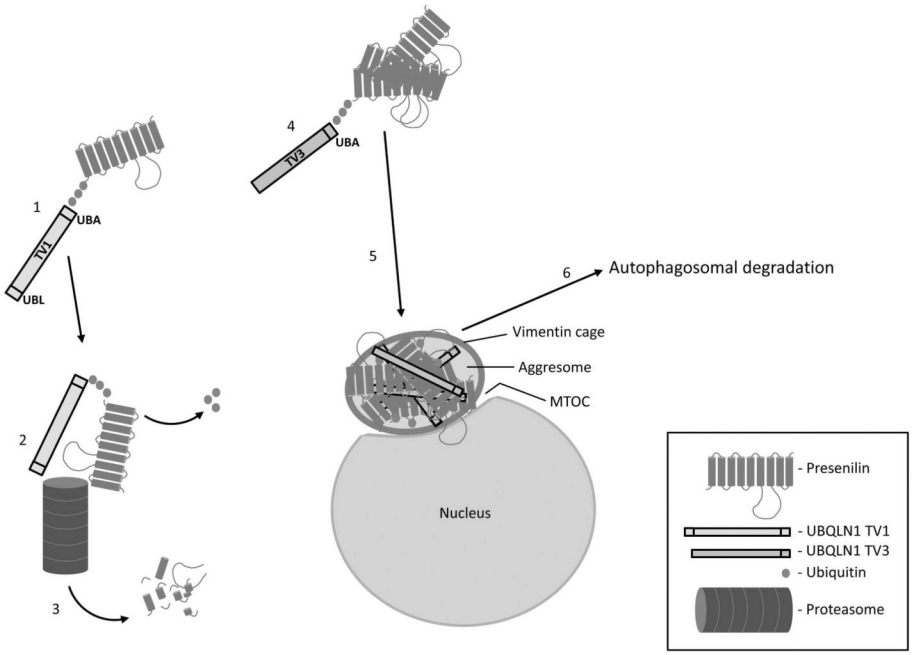

Figure 12. Potential role of ubiquilin-1 TV1 and TV3 in proteasomal degradation and aggresomal accumulation of PS1

1. TV1 binds poly-ubiquitinated PS1 destined for degradation via its UBA domain. 2. TV1 takes PS1 to the proteasome. The interaction of TV1 with the proteasome is mediated by its UBL domain. 3. PS1 is degraded by the proteasome. 4. TV3 binds poly-ubiquitinated PS1 in the same way as TV1. However, since it lacks most of the UBL domain, TV3 does not efficiently bind to the proteasome, resulting in the accumulation of TV3-PS1 complexes in the cell. 5. Accumulated TV3-PS1 complexes are sequestered to the juxtanuclear MTOC as vimentin-caged aggresomes, rendering the possibly toxic accumulated proteins harmless. 6. The aggresome may be directed for autophagosomal degradation.

TABLE 1

FRET between ubiquilin-1 V5 and PS CT in CHO cells over-expressing PS1 and ubiquilin-1 TV1 or TV3

FRET DONOR (ALEXA 430)	FRET ACCEPTOR (Cy3)	ALEXA 430 LIFETIME (mean ± SD, psec)	FRET STRENGTH
TV1	none	4070 ± 349	0
TV1	PS1 CT	1494 ± 89	0.45 ± 0.07
TV3	none	3773 ± 163	0
TV3	PS1 CT	1349 ± 145	0.3 ± 0.06